Multi-Coloured Sequential Resonance Energy Transfer for Simultaneous Ligand Binding at G Protein-Coupled Receptors

Alice Valentini[1], Bethany Dibnah[2], Marija Ciba[1], Trond Ulven[1], Brian D. Hudson[2]* and Elisabeth Rexen Ulven[1]*

1. Department of Drug Design and Pharmacology, University of Copenhagen, Universitetsparken 2, DK-2100 Copenhagen, Denmark.
2. Centre for Translational Pharmacology, School of Molecular Biosciences, College of Medical, Veterinary and Life Sciences, University of Glasgow, Glasgow G12 8QQ, Scotland United Kingdom.

***** To whom correspondence should be addressed

Abstract

G protein coupled receptors (GPCRs) are the largest family of signalling proteins and highly successful drug targets. To date, most GPCR drugs interact with the binding pocket for the natural ligand, typically near the extracellular part of the transmembrane region. Recent advancements in structural biology have identified additional allosteric binding sites in other parts of these receptors. Allosteric sites provide several theoretical advantages, including the ability to modulate natural ligand function, and there is a need for better ways to study how ligands bind and interact with different GPCR binding sites. We have developed an approach to study multiple ligands binding to the same receptor based on sequential resonance energy transfer between two fluorescent ligands bound simultaneously to a GPCR. We use this approach to gain insight into allosteric ligand interactions for a clinically relevant receptor. This method will provide important information to aid development of new GPCR drugs.

Introduction

G protein coupled receptors (GPCRs) are the most successful drug targets, with estimates suggesting one third of drugs act through this family.[1] The success of GPCRs derives from their diverse biology and from our understanding of how to develop drugs that interact with these receptors. GPCRs share a conserved seven transmembrane structure, which allows them to transmit signals from extracellular ligands, including hormones, neurotransmitters and metabolites, into intracellular responses. These physiological GPCR ligands interact with the orthosteric binding site, which is most commonly found at the top of the transmembrane helical bundle.[2] Traditional GPCR drug discovery has had great success identifying synthetic ligands that compete for binding at these orthosteric sites, however recently, focus has shifted towards developing drugs that produce effects by binding to distinct allosteric sites.[3]

Allosteric GPCR ligands provide conceptual advantages over orthosteric ligands. While orthosteric ligands primarily function as either partial or full agonists, acting in a similar way to the physiological ligand, or antagonists, competing for binding with the physiological ligand; allosteric ligands may affect receptor function in more diverse ways.[4] Specifically, while some allosteric ligands function as agonists directly activating their receptor, more commonly, allosteric ligands affect receptor function by modulating the way physiological ligands bind to and initiate signalling through the receptor.[5] This means that allosteric modulators have a saturable effect, reducing the risk of adverse response, and will either enhance or supress function, while maintaining natural spatiotemporal control of signalling.[6] Attention has also been given to the possibility that allosteric ligands may bias signalling towards particular pathways,[7] allowing for a more fine-tuned control of signalling. While this diversity in allosteric ligand function creates opportunity to develop novel GPCR drugs, it also presents challenges to how we measure the unique effects these ligands have.

The revolution in GPCR structural biology led by advances in X-ray crystallography and cryogenic electron microscopy has made it possible to define the locations where allosteric ligands bind to GPCRs.[8] These locations have proven diverse, with examples of allosteric ligands binding both to extracellular facing pockets and to extrahelical pockets facing the lipid bilayer. While these structural approaches are invaluable, they must be complimented with functional approaches able to define the effects these ligands have. Considering that allosteric ligands produce their effects in part by modulating the binding affinity and kinetics of ligands binding to other sites on the receptor, developing novel approaches able to measure and quantify simultaneous binding of multiple ligands to the same receptor would be of real value.

Resonance energy transfer approaches including bioluminescence and Förster resonance energy transfer (BRET and FRET) are highly effective at measuring binding of fluorescently labelled ligands to GPCRs.[9] In particular, the development of NanoBRET, which measure energy transfer from a nanoluciferase (Nluc) fused to the extracellular N terminal of the GPCR to a fluorescent ligand,[10] has revolutionised GPCR ligand binding studies. However, no method exists for probing the dynamic interplay between multiple ligands simultaneously interacting with a receptor. An approach to achieve this would be to combine multiple fluorescent ligands with overlapping spectral properties, allowing for sequential energy transfer from an Nluc tag to a fluorescent ligand binding at one site, then subsequent energy transfer to a second fluorescent ligand binding to a different site.

Such an approach would allow for the direct measurement of ligand binding parameters including affinity and binding kinetics only from receptors with both fluorescent ligands simultaneously bound.

To demonstrate the potential of this approach, we characterise ligand binding to the free fatty acid receptor FFA1, a clinically important GPCR with potential in the treatment of metabolic disorders.[11] The pharmacology of ligand binding to FFA1 is complex, with studies demonstrating at least two distinct allosteric sites on the receptor that each show cooperativity with fatty acid binding.[12] Structural studies established that one of these sites, often referred to as allosteric site one, resides near the traditional GPCR orthosteric site, but extends out of the helical core through a gap between TM3 and TM4.[13] Adding complexity, recent cryo-EM structures bound to fatty acid ligands suggested that this site is at least one site were fatty acids bind to the receptor.[14] The second binding site, often referred to as allosteric site two, is a lipid facing extrahelical pocket formed between the bottoms of TM3, TM4, TM5 and intracellular loop 2.[15] Ligands binding to allosteric site two are notable for having greater efficacy and therefore site one and site two ligands are sometimes referred to as partial and full FFA1 agonists, respectively.[11] Previous work has shown that NanoBRET can effectively measure ligand binding to FFA1 site one,[16] while no fluorescent tracers have been reported for site two. We have developed tracers binding to each of these two sites possessing fluorescent properties optimised for sequential resonance energy transfer.[17] These ligands are combined with NanoBRET to simultaneously measure binding to multiple sites on the FFA1 receptor.

Results

Development of a fluorescent tracer binding to FFA1 site two

To establish a resonance energy transfer-based method to measure simultaneous ligand binding to FFA1, suitable tracers with affinity for both FFA1 binding sites are required. High affinity fluorescent tracers for site one are known,[16, 18, 19] but no fluorescent tracers have been described that bind to site two. Given the structural similarities among ligands binding to the two FFA1 sites,[12] it was critical to employ a screening strategy that could confirm the binding site of novel tracers. Since site two FFA1 ligands behave as full agonists in Gαq signalling, while site one ligands are partial agonists, a Gαq-based FFA1 Ca^{2+} mobilisation assay was employed. Two reference site two compounds, T-3601386 (T360)[20] and Cpd 6h,[21] show full agonism, while a reference site one compound, TUG-770,[22] exhibited partial agonism (**Sup. Table 1**). To identify potential attachment sites and suitable linkers for fluorophore labelling, Cpd 6h served as template for the design of a series of analogues linked to a Boc-amine that were synthesized and screened (**Sup. Table 1**). This follows a strategy previously used, where the Boc-amine serves as a stable steric probe that, if tolerated, is deprotected and coupled to the desired fluorophore.[23] All compounds showed FFA1 full agonism, consistent with binding to site two. Two compounds were identified with nanomolar potency and the best scope for conversion to fluorescent tracers, TUG-2457 and TUG-2467.

To generate green fluorescent tracers, a nitrobenzofurazan (NBD) fluorophore was incorporated into TUG-2457 and TUG-2467 to produce the putative tracers TUG-2489 and

TUG-2490 (**Fig. 1A**). While both compounds show full agonist activity at FFA1 (**Fig. 1B**; **Sup. Table 1**), their potencies were low ($EC_{50:}$ 0.8-4 μM) suggesting they likely bind with low affinity. As TUG-2490 displayed higher potency, we aimed to further improve this compound by replacing its phenyl substituent with a 6-methyl-2-pyridyl, as is present in Cpd 6h, resulting in TUG-2597 (**Fig. 1A**). Pleasingly, TUG-2597 has a much-improved potency of 73 nM, while maintaining full agonist activity (**Fig 1B**; **Sup. Table 1**). In addition, introduction of the heterocycle improved aqueous solubility, which was a limiting factor with the two previous analogues. To explore alternative sites for fluorophore addition, we also produced TUG-2598 (**Fig. 1A**), a derivative where the NBD fluorophore has been linked to the carboxylate of Cpd 6h, which according to the crystal structure does not participate in any ionic interactions.[15] Unfortunately, this modification resulted in a loss of activity (**Fig. 1B**), and therefore we proceeded with TUG-2597 as the best FFA1 site two tracer.

To use TUG-2597 in a NanoBRET-based binding assay, a version of FFA1 tagged with the Nanoluciferase (Nluc) BRET energy donor is required. Traditionally, NanoBRET GPCR binding assays employ receptors tagged at their N terminal, resulting in proximity to extracellular facing orthosteric sites.[10] However, binding site two of FFA1 resides within an extrahelical groove located near intracellular loop 2,[15, 24] and depending on where the fluorophore is attached on the ligand and the nature and length of the linker, it is not obvious whether a tracer binding to this site would be in closer proximity to an N or the C terminal Nluc tag. The NBD of TUG-2597 is predicted to be situated in the middle of the membrane, sufficiently close for BRET to occur with either Nluc location (**Fig. 1C**). After confirming that the function of TUG-2597 was not affected by Nluc at either location (**Fig. 1D**), saturation NanoBRET binding experiments confirmed that binding of TUG-2597 (K_d= 350-440 nM) could be measured using either receptor construct (**Fig. 1E-F**). Direct comparison of BRET signals measured confirmed our prediction that more efficient energy transfer would occur using the N terminal Nluc location (**Fig. 1G**).

Development of an FFA1 site one red fluorescent tracer

Having identified a green tracer for site two, we next set out to identify a suitable red tracer binding to FFA1 site one. To be used in simultaneous sequential energy transfer with TUG-2597, the compound needs to both bind with high affinity and contain a fluorophore that could serve as FRET acceptor for the NBD in TUG-2597. We initially generated two putative red tracers based on a previously published FFA1 NBD containing tracer,[16] one with the red sulfo-cyanine5 (SulfoCy5), TUG-2355, and one with the orange-red emitting Cy3.5, TUG-2287 (**Fig. 2A**). When tested in Ca^{2+} assays (**Sup. Table 1**), TUG-2355 retained activity (**Fig. 2B**), but showed poor potency while TUG-2287 displayed no measurable activity. To improve the SulfoCy5 tracer we designed a compound with shortened linker on either site of the amide connector, TUG-2591 (**Fig. 2A**), and were pleased to see a marked improvement in potency (**Fig. 2B, Sup. Table 1**). All three red tracers showed comparable activity when tested at N and C terminal Nluc receptor fusions (**Fig 2. C-D**).

In NanoBRET binding assays using the N terminal Nluc-FFA1 construct (**Fig. 2F-H**), the results for the two SulfoCy5 compounds were as predicted, TUG-2591 displayed higher affinity than TUG-2355. Unexpectedly, the Cy3.5 compound, TUG-2287, which was inactive in Ca^{2+} assays displayed the highest affinity. These observations suggest the

Cy3.5 fluorophore in TUG-2287 interferes with the intrinsic activity of the compound, resulting in a compound with affinity but no agonism. Importantly, across all three site one red tracers little to no specific BRET was measured when using the C terminal FFA1-Nluc fusion (**Fig. 2F-H**), indicating that site one is too far away from the C terminal Nluc for efficient resonance energy transfer.

DISCo-BRET measures simultaneous ligand binding to distinct FFA1 sites

To measure simultaneous ligand binding to FFA1, a sequential resonance energy transfer approach has been employed. There is excellent spectral overlap between the emission of Nluc and the excitation of our green tracer, TUG-2597, as well as overlap between the emission of TUG-2597 and the excitation of our red tracer, TUG-2591 (**Fig. 3A**). This suggests sequential resonance energy transfer from Nluc to the green TUG-2597, then on to the red TUG-2591 may occur if both compounds are binding FFA1 simultaneously. However, given the broad emission peak of Nluc, and potential for direct BRET between Nluc and TUG-2591 (**Fig. 2F**), we hypothesised that incorporating physical separation between Nluc, and the red TUG-2591, which can be bridged by the green TUG-2597, would contribute to energy acceptance from the green fluorophore rather than directly from Nluc. We have achieved this by using an FFA1 construct with Nluc at the intracellular C terminal of the receptor, and by incorporating a hydrophilic SulfoCy5 fluorophore into the red tracer, TUG-2591. Considering the location of site one, the hydrophilic SulfoCy5 should remain outside of the lipid bilayer and therefore sufficiently separated from the C terminal Nluc. Further, given that the green TUG-2597 binds to an extrahelical site within the bilayer, we predict that this should provide the optimal condition for multi-coloured Dual Interaction Sequential Compounds (DISCo)-BRET, measuring energy transfer from the intracellular Nluc, through green TUG-2597 and on to red TUG-2591 (**Fig. 3B**).

To measure DISCo-BRET, cells expressing FFA1 tagged at its N (**Fig. 3C**) or C (**Fig. 3D**) terminal with Nluc were incubated in increasing concentrations of the red site one tracer, in the absence or presence of the green site two tracer. Luminescent emission spectra were obtained, confirming that in the absence of green tracer, specific BRET emission from the red tracer was observed at 690 nm when using the N terminal Nluc construct (**Fig. 3Ci-Cii**). In contrast, little BRET was observed with the C terminal Nluc construct (**Fig. 3Di-Dii**). Addition of the green tracer, resulted in a clear increase in BRET at 540 nm using either the N (**Fig. 3Ciii**) or C (**Fig. 3Diii**) terminal construct, indicative of direct BRET from Nluc to this tracer. Critically, addition of the green site two tracer also resulted in a clear increase in emission at 690 nm from the red site one tracer, again when using either the N (**Fig. 3Ciii-Civ**) or C (**Fig. 3Diii-Div**) terminal Nluc construct. To quantify this sequential energy transfer, we measured the area under the two emissions peaks, plotting the ratio as a saturation binding curve for the red tracer, TUG-2591 (**Fig. 3E-3F**). These experiments demonstrate specific DISCo-BRET can be measured using either the N or C terminal construct, yielding K_d values for TUG-2591 of 50-100 nM. However, to simplify the experiment, we also measured DISCo-BRET by discretely measuring luminescent emission at three wavelengths, corresponding to Nluc, NBD and SulfoCy5 and plotting ratios of these emissions (**Sup. Fig. 1**). These data demonstrate that while DISCo-BRET can be measured using simple BRET ratios, significant direct BRET between Nluc and TUG-2591 when using the Nluc-FFA1 construct, makes it difficult to distinguish green tracer dependent DISCo-BRET from green tracer independent direct BRET (**Sup.**

Fig. 1A). In contrast, green tracer dependent DISCo-BRET was easily established using the FFA1-Nluc construct (**Sup. Fig. 1B**), in line with our prediction (**Fig. 3B**). Although we found DISCo-BRET could be effectively measured using either the ratio of SulfoCy5/Nluc (**Sup. Fig. 1Bi**) or SulfoCy5/NBD (**Sup. Fig. 1Biii**) emission wavelengths, we have chosen to use the SulfoCy5/NBD ratio for further experiments.

DISCo-BRET Differentiates FFA1 ligands based on Binding Site

To demonstrate the potential of DISCo-BRET to characterise FFA1 ligands, a selection of previously reported compounds was tested in competition binding studies. These ligands included a mixture of site one compounds: TUG-905,[25] TUG-770,[22] TAK-875,[26] and Merck Cpd-B;[27] one long chain fatty acid, α-linolenic acid (aLA); two site two compounds, T360[20] and Cpd 6h;[21] and one antagonist with unclear binding site, GW1100.[28] DISCo-BRET binding studies were carried out with cells incubated with both the red and the green tracers along with increasing concentrations of the competing ligand. DISCo-BRET was measured using the SulfoCy5/NBD ratio (**Fig. 4A**), while binding of the green tracer was monitored using the NBD/Nluc ratio (**Fig. 4B**). BRET spectra were also obtained for each competing ligand to visualise DISCo and direct BRET (**Sup. Fig. 2**). All site one ligands resulted in complete competition of DISCo-BRET, indicative of competitive binding with the red tracer (**Fig. 4Ai**). These site one ligands also enhanced binding of the site two green tracer, consistent with cooperativity between agonists binding at FFA1 site one and site two (**Fig. 4Bi**). Clear differences in affinity across these compounds were observed, where TUG-905 > TAK-875 > TUG-770 > Cpd-B (**Sup. Table 2**). The fatty acid ligand, aLA, produced only a modest DISCo-BRET competition (**Fig. 4Ai**), and slight enhancement of green tracer binding (**Fig. 4Bi**), likely due to low affinity for fatty acids at either site one or site two. In contrast, the site two compounds, T360 and Cpd 6h, display clear competition in both DISCo-BRET and green tracer binding (**Fig. 4Aii and 4Bii**). It is notable that these compounds did not result in complete competition of the DISCo-BRET (**Fig 4. Aii; Sup. Table 2**), likely due to a low-level of direct BRET from the C terminal Nluc to the red tracer. The fact that T360 and Cpd 6h show competition in DISCo-BRET can only be explained by the ability of these ligands to displace the green tracer and therefore disrupt the sequential energy transfer on to the red tracer TUG-2591, and the residual BRET can only be explained by T360 and Cpd 6h binding to site two rather than directly competing with TUG-2591. Thus, the low-level direct energy transfer from Nluc to the red tracer confirms the binding site of the non-fluorescent ligand. Supporting this, separate NanoBRET competition binding assays using Nluc-FFA1 demonstrate that both T360 and Cpd 6h actually have positive cooperativity with the red tracer (**Fig. 4Ci; Sup. Table 3**). As expected, NanoBRET binding assays for the green tracer (**Fig. 4Cii; Sup. Table 3**) show broadly the same pattern of competition/enhancement as observed for this tracer when measuring the NBD/Nluc ratio in the dual tracer DISCo-BRET assay (**Fig. 4B; Sup. Table 3**). It was also notable that the FFA1 antagonist, GW1100, showed no competition or enhancement for either the DISCo-BRET (**Fig. 4Aii**) or green tracer binding (**Fig. 4Bii**), suggesting that this antagonist binds a site distinct from either site one or two.

Allosteric Regulation of FFA1 Ligand Dissociation

To assess how allosteric interactions affect ligand binding kinetics, we first aimed to determine allosteric effects on the dissociation binding kinetics of our red tracer, TUG-

2591, and the green tracer, TUG-2597. Both tracers were co-added to monitor association, followed by the addition of high concentrations of competing ligands for either site one or site two to stimulate dissociation from one, the other, or both sites (**Fig. 5A**). Tracer binding was monitored as either DISCo-BRET to assess binding of the red tracer (**Fig. 5B**), or as NBD/Nluc to measure binding of the green tracer (**Fig. 5C**). Comparison of the DISCo-BRET dissociation curves obtained with different displacing ligands allowed for the determination of off-rate kinetics of each ligand, specifically from receptors bound to both ligands simultaneously (**Fig. 5D and Sup. Table 4**). It was notable that the off-rate for the red TUG-2591 from site one was substantially slower than that of the green TUG-2597 from site two. Comparing the overall dissociation rate for our green tracer (**Fig. 5E**), obtained using the NBD/Nluc ratio (accounting for FFA1-Nluc co-bound with red TUG-2591 or not), suggested that the dissociation rate for the green tracer is broadly the same as when measured only from receptors co-bound to the red tracer (**Sup. Table 4**). To further confirm that the red TUG-2591 does not affect the green TUG-2597 dissociation rate, association/dissociation experiments for our green site two tracer were carried out in single ligand NanoBRET format (**Fig. 5G**), which demonstrated a similar off-rate (**Sup. Table 4**). While these data suggest the dissociation rate of our green site two tracer is not greatly affected by red tracer binding, the relatively slow DISCo-BRET dissociation rate for the red tracer led us to also examine the binding kinetics of this tracer in a single ligand NanoBRET format (**Fig. 5H**). Surprisingly, these experiments demonstrate that the off-rate of our red tracer is approximately 10 times faster for the single ligand experiment compared with the DISCo-BRET experiment (**Sup. Table 4**). These findings demonstrate that DISCo-BRET can define how ligand binding to one site of a GPCR will affect the dissociation rate at a second site.

Allosteric Regulation of FFA1 Ligand Association

Having demonstrated the potential for DISCo-BRET to study dissociation kinetics, we next explored association binding. Cells were first incubated with our red tracer, TUG-2591, followed by addition of the green tracer, TUG-2597 (**Fig. 6A**). Binding was then assessed either using the DISCo-BRET SulfoCy5/NBD ratio (**Fig. 6B**), or the NBD/Nluc ratio measuring binding of the green tracer (**Fig. 6C**). As expected, little increase in SulfoCy5/NBD BRET was seen following incubation with our red tracer, while a rapid increase was observed following addition of green tracer (**Fig. 6B**). All DISCo-BRET was blocked by pre-treatment with a site one competing ligand, TUG-905. When assessing site two ligand binding, association was observed after addition of green TUG-2597 alone, which was enhanced by the presence of TUG-905, consistent with positive cooperativity between these ligands. Analysis of the DISCo-BRET association rate observed upon addition of TUG-2597 compared with the rate observed from NBD/Nluc, and with the association rate of TUG-2597 from a single ligand NanoBRET experiment, indicated that all three rates were identical (**Sup. Fig. 3A; Sup. Table 5**). This indicates DISCo-BRET association observed is due to green TUG-2597 binding at site two to receptors that were pre-bound to the red tracer at site one. The fact that the single ligand experiment also shows a similar association rate, indicates that the association rate of green TUG-2597 is not affected by red TUG-2591 binding. This was further confirmed by single ligand NanoBRET association studies using multiple concentrations of green tracer (**Sup. Fig 3B**), again showing broadly similar association kinetics (**Sup. Table 5**).

Finally, to examine how binding of green TUG-2597 to site two affects binding of red TUG-2591 to site one, experiments were conducted where the green tracer was added first, followed by the addition of the red tracer (**Fig. 6D**). As before, binding of green tracer was measured using the NBD/Nluc BRET ratio (**Fig. 6F**), while binding of the red tracer was assessed through DISCo-BRET and SulfoCy5/NBD ratio (**Fig. 6E**). These results demonstrated a rapid binding of green tracer, which was not impacted by the addition of red tracer, although green tracer binding was enhanced by pre-treatment with the site one competing compound, TUG-905 (**Fig. 6E**). Addition of red tracer did however lead to a clear increase in DISCo-BRET, but notably this occurred with a relatively slow association rate (**Fig. 6F; Supp. Table 5**). To clearly define the association rate of our red tracer at FFA1 receptors pre-bound to green TUG-2597, DISCo-BRET association experiments were conducted pre-treating with the green tracer, followed by addition of multiple concentrations of red tracer (**Fig. 6G**). Isolation of the red TUG-2591 association kinetics allowed for calculation of binding parameters that are broadly in line with those calculated from the single concentration experiment (**Fig. 6H; Sup. Table 5**). However, when comparable NanoBRET binding was used to assess the association kinetics of red TUG-2591 in the absence of green TUG-2597, substantially faster association rates were observed (**Fig. 6I; Sup. Table 5**). Indeed, the association rate of this tracer was approximately ten times slower when measured using DISCo-BRET to assess binding to receptors already bound with green TUG-2597, than it was when binding to a ligand free receptor. Interestingly, this broadly corresponds to the reduction in off rate seen for red TUG-2591 when green TUG-2597 is bound, and as a result the overall affinity of TUG-2591 for site one remains largely unchanged regardless of whether green TUG-2597 is bound to site two or not (**Sup. Table 5**). These data demonstrate that while green TUG-2597 binding to site two does not alter the affinity of red TUG-2591 for site one, it does alter the binding kinetics.

Discussion

GPCRs are the largest and most important family of drug targets. In recent times significant focus on these receptors has shifted towards developing ligands that interact with allosteric sites, distinct from the binding site of the physiological ligand for the receptor.[5] We have developed a novel multi-coloured BRET approach that allows for simultaneous measurement of ligand interaction at multiple GPCR binding sites. We demonstrate that this approach can be used to understand which ligands bind to particular sites and to define how ligands interact with each other to affect affinity and kinetics.

BRET as a technology has become an invaluable tool in GPCR research and BRET biosensors have been developed to measure nearly every aspect of GPCR function.[29] NanoBRET based binding assays have in particular provided opportunity for improved GPCR ligand binding studies.[10] While advancements in NanoBRET have allowed this approach to explore binding to receptor oligomers,[30] or to measure binding to intracellular binding sites,[31] to date it has not been possible to use NanoBRET to study binding to multiple sites on the same receptor, at the same time. To achieve this, we have employed a multi-colour sequential BRET strategy that we name DISCo-BRET. Historically, multi-colour BRET protein-protein interaction studies have focused on multiplex strategies, where a single luciferase separately donates energy to two different

acceptors.[32, 33] While this is useful, it does not require both acceptors to be present for final acceptor emission, and therefore does not allow measurement only when the donor and both acceptors are all in close proximity. Employing sequential resonance energy transfer, where energy passes from donor to a first acceptor, which then transfers energy to the final acceptor addresses this issue. However, very few studies have successfully employed sequential energy transfer BRET, even when measuring protein-protein interactions, with the best example having used the approach to demonstrate a heterotrimer among three GPCRs.[34]

The biggest challenge to sequential resonance energy transfer is the wide emission band of luciferase enzymes, making it difficult to find a final energy acceptor that does not directly accept energy from the luciferase. Indeed, when developing NanoBRET assays, it has often been recommended to use red and far red tracers, despite these fluorophores having relatively little spectral overlap with Nluc because they give a lower background.[9, 35] To overcome this issue, we have taken advantage of both the physical separation between two different GPCR allosteric binding sites, as well as the chemical properties of different fluorophores. This has allowed us to develop the DISCo-BRET assay where it is the physical separation between the Nluc energy donor and the final red fluorophore acceptor across the cell membrane that dictates the requirement for an intermediator ligand. While we have employed this approach to study the FFA1 receptor, given that there are increasing numbers of structures showing GPCR ligands binding to extrahelical allosteric binding sites,[8] we anticipate our approach can be adapted to study many other GPCRs.

FFA1 is a clinically relevant GPCR with potential for the treatment of diabetes or other metabolic disorders.[11, 36] Importantly, there is also clear evidence that FFA1 ligands binding to the two sites have different biological effects.[37] By helping to understand how these two binding sites interact with each other, we are likely to open new opportunities for future FFA1 ligand development. In examining the interactions between our FFA1 site one and site two tracers, it was particularly notable that while the binding kinetics was altered for the site one tracer, there was no effect on binding kinetics for the site two tracer. A central principle of allosteric ligand modulation is that it must be reciprocal between the two ligands.[38] While our findings suggest that this is true in relation to the ultimate binding affinity, which was not affected for either ligand, the effect on kinetics was clearly not equivalent between the two ligands. Given the structure of the FFA1 site one,[13] and likely ligand entry through an opening accessed via the lipid, the altered kinetics we observe perhaps suggest binding of the site two ligand impacts access through the opening.

In summary, we have developed a novel approach to measure simultaneous ligand engagement with multiple GPCR binding sites. We have used this to better understand ligand interaction with FFA1, a clinically validated drug target, and our new approach will help provide new key insights to the future of allosteric GPCR drug discovery.

Methods

Chemical Synthesis

All compounds were synthesised as described in the Supplemental Methods. The identity of synthesised compounds was confirmed by NMR and HRMS and all compounds used were shown to have a minimum of 95% purity.

Plasmids

A plasmid containing the FFA1 sequence fused in frame at its C terminal to Nluc was generated in the pcDNA5 FRT/TO (ThermoFisher Scientific, UK) plasmid backbone. The sequence for the human FFA1 receptor without its stop codon was inserted between HindIII and KpnI sites, while the Nluc sequence inserted between KpnI and XhoI sites in the parental plasmid. After ligation, and transformation, the identity of the resulting plasmid was confirmed by sequencing (University of Dundee Sequencing Service).

Cell culture and transfections

All Flp-In T-REx 293 cell lines were maintained in Dulbecco's Modified Eagles Medium (DMEM), supplemented with 10% foetal bovine serum, penicillin/streptomycin and normocin (InvivoGen, UK). Cells were cultured at 37 °C and 5% CO_2 in a humidified atmosphere and subcultured as required. The Nluc-FFA1 Flp-In T-REx 293 cell line, inducibly expressing the FFA1 receptor fused at its N terminus to Nluc, was as described previously.[16] The FFA1-Nluc Flp-In T-REx 293 cell line, inducibly expressing the FFA1 receptor fused at its C terminus to Nluc, was generated by first using polyethylenimine to co-transfect parental Flp-In T-REx 293 cells (ThermoFisher Scientific, UK), with the FFA1-Nluc plasmid and a POG44 plasmid (ThermoFisher Scientific, UK), expressing an Flp recombinase. Following transfection, cells were selected using blasticidin and hygromycin B to obtain an isogentic cell line with FFA1-Nluc incorporated into the Flp recombinase site. For all experiments with Flp-In T-REx 293 cell lines, cells were treated with 100 ng/ml of doxycycline for 24 h to induce expression of the transfected construct.

Ca^{2+} mobilisation

Nluc-FFA1 or FFA1-Nluc Flp-In T-REx 293 cells were plated at 50,000 cells per well in poly-D lysine coated black clear bottom 96-well plates. Cells were then cultured for 24 h until reaching confluency before culture medium was replaced with medium containing 100 ng/ml of doxycycline to induce receptor expression. Cells were cultured for a further 24 h before the assay. On the day of the assay culture medium was removed and replaced with medium containing 3 μM Fura2-AM Ca^{2+} dye. Cells were returned to the cell culture incubator for 45 min before medium and dye removed, and cells washed twice with Hanks Balanced Salt Solution supplemented with 20 mM HEPES (HBSS). After washing cells were incubated in HBSS for 15 min at 37 °C before being transferred to a Flexstation micro-plate reader (Molecular Devices). Fura2 fluorescent emission at 520 nm following excitation with each of 340 and 380 nm was measured in regular intervals both before and after adding test compounds for a total of 90 s per well. Calcium responses were determined by taking the peak 340/380 ratio after first subtracting the ratios obtained prior to addition of test compound.

NanoBRET

Nluc-FFA1 or FFA1-Nluc Flp-In T-REx 293 cells were plated at 50,000 cells per well in poly-D lysine coated white 96-well plates. Cells were cultured for 24 h in the plate before medium was replaced with medium containing 100 ng/ml of doxycycline to induce receptor expression. After culturing for a further 24 h, medium was removed, cells washed with HBSS and incubated in HBSS for 30 min. To start the assay, NanoGlo substrate (Promega) was added to the cells at a 1:800 final dilution and incubated for 10 min at 37 °C. For endpoint assays, including both saturation and competition binding, test ligands were then added, including both fluorescent and unlabelled competing ligands as indicated, and plates incubated for a further 5 min at 37 °C. NanoBRET was then quantified in a CLARIOstar microplate reader (BMG Labtech) by measuring luminescent emission with the monochrometer set for the Nluc donor at 450 - 60 nm, and acceptor luminescent emission 540 - 60 nm (NBD), 600 - 80 nm (Cy3.5) or 690 – 100 nm (SulfoCy5), depending on which fluorophore was being tested. The acceptor/donor BRET ratio was then taken as a measure of fluorophore binding. For kinetic on then off NanoBRET experiments plates were washed the same way and substrate was added to the same concentration. However, 10 min after substrate was added plates were inserted into the CLARIOstar microplate reader set to 25 °C to take repeated measurements of luminescent emission for both the donor and the acceptor fluorophore being used. After 5 min of background measurements, the indicated concentration of fluorescent ligand was added using the plate reader injector and luminescent emission was monitored for approximately 10 min before the reader was paused to manually add a high concentration of appropriate competing ligand to initiate dissociation. The plate was returned to the reader and luminescence measurements were continued for a further 30 min to monitor dissociation of the fluorescent ligand. For kinetic experiments using multiple concentrations of fluorescent ligand, cells were placed in the plate reader immediately after the addition of Nano-Glo substrate and luminescent measurements were taken. After 5 min, the reader was paused to add the indicated concentrations of fluorescent ligand, before measurements were continued. To set non-specific binding for kinetic experiments, the indicated competing ligand was added 5 min before the addition of the fluorescent ligand.

DISCo-BRET

Nluc-FFA1 or FFA1-Nluc Flp-In T-REx 293 cells were plated at 50,000 cells per well in poly-D lysine coated white 96-well plates. Cells were cultured for 24 h in the plate before medium was replaced with medium containing 100 ng/ml of doxycycline to induce receptor expression. After culturing for a further 24 h, culture medium was removed, cells washed with HBSS and incubated in HBSS for 30 min. For all DISCo-BRET formats Nano-Glo substrate was then added at a 1:800 final dilution and cells incubated for 10 min. Following substrate addition experimental set up different among the three formats: endpoint, spectra scan, and kinetics.

For endpoint experiments all fluorescent and unlabelled ligands were added to the cells and incubated for 5 min at 37 °C. Luminescent emission was then measured using a CLARIOstar microplate reader with monochromator set at 450 - 60 nm (Nluc), 540 - 60 nm (NBD) and 690 - 100 nm (SulfoCy5). BRET ratios were then calculated as either

SulfoCy5 emission divided by NBD emission, SulfoCy5 emission divided by Nluc emission, or NBD emission divided by Nluc emission.

For spectra scan experiments all indicated fluorescent and unlabelled ligands were added to the cells and cells incubated for 5 min at 37 °C. Luminescence emissions were then measured from each well of the plate from 440 nm – 740 nm with a 5 nm resolution using a CLARIOstar microplate. Luminescent emission spectra were then normalised as a percentage of the maximal Nluc emission peak (~460 nm), then subtracted with the spectrum obtained in the presence of high concentrations of ligands competing for both binding sites to obtain specific BRET binding spectra.

In kinetic DISCo-BRET experiments plates were placed directly in a CLARIOstar plate reader set to 25 °C 10 min after Nano-Glo substrate addition. Luminescent measurements were then taken with three sequential measurements per well with the monochromator set to 450 - 60 nm (Nluc), 540 - 60 nm (NBD) and 690 - 100 nm (SulfoCy5) taken in 20 or 30 s intervals. After 5 min of background measurements, the plate reader was paused for the first indicated fluorescent ligand(s) addition, before immediately returning the plate to the reader to continue luminescence readings. After 5 min, the reader was again paused to add the second fluorescent ligand (association assays) or competing ligand(s) (dissociation assays), before immediately continuing the measurements for the indicated time. Non-specific control binding was obtained by adding the indicated competing ligand(s) 5 min prior to the addition of the first fluorescent ligand.

Data Analysis

All data presented are mean ± SEM from a minimum of three independent experiments. Data analyses and curve fitting were carried out using Graphpad Prism 10 (GraphPad Software, USA). For all concentration response experiments, data were fit to a three-parameter log agonist concentration vs response model, where the vehicle treatment was plotted at one log unit lower than the lowest tested concentration. Saturation, displacement and kinetic binding data were fit to models as is indicated in the respective figure legends.

Acknowledgements

This work was supported by the Lundbeck Foundation (ERU, grant no. R307-2018-2950), the Academy of Medical Sciences (BDH, grant no. SBF004\1033) and Tenovus Scotland (BDH, grant no S18-20). We would also like to recognise Elaine Duncan for her input in developing the DISCo-BRET assay name, Matjaz Brvar and Christoffer V. Heidtmann for help with synthesis of fluorescent building blocks, and Junsheng Chen for help with recording fluorescence spectre.

Author Contributions

The project was conceived by ERU, and funding secured by ERU and BDH. AV, supervised by ERU, and MC, supervised by ERU and TU, carried out all chemical synthesis and characterisations. AV, BD and BDH completed all biological experiments and data analysis, including for Ca^{2+} and BRET based experiments, supervised by BDH. All authors contributed to the writing of the manuscript.

References:

1. Hauser, A.S., Attwood, M.M., Rask-Andersen, M., Schioth, H.B. & Gloriam, D.E. Trends in GPCR drug discovery: new agents, targets and indications. *Nat Rev Drug Discov* **16**, 829-842 (2017).
2. Congreve, M., de Graaf, C., Swain, N.A. & Tate, C.G. Impact of GPCR Structures on Drug Discovery. *Cell* **181**, 81-91 (2020).
3. Wootten, D., Christopoulos, A. & Sexton, P.M. Emerging paradigms in GPCR allostery: implications for drug discovery. *Nature Reviews Drug Discovery* **12**, 630-644 (2013).
4. Kenakin, T. Theoretical Aspects of GPCR-Ligand Complex Pharmacology. *Chem Rev* **117**, 4-20 (2017).
5. Felder, C.C. GPCR drug discovery-moving beyond the orthosteric to the allosteric domain. *Advances in pharmacology* **86**, 1-20 (2019).
6. Conn, P.J., Lindsley, C.W., Meiler, J. & Niswender, C.M. Opportunities and challenges in the discovery of allosteric modulators of GPCRs for treating CNS disorders. *Nat Rev Drug Discov* **13**, 692-708 (2014).
7. Slosky, L.M., Caron, M.G. & Barak, L.S. Biased Allosteric Modulators: New Frontiers in GPCR Drug Discovery. *Trends Pharmacol Sci* **42**, 283-299 (2021).
8. Zhang, L., Mobbs, J.I., May, L.T., Glukhova, A. & Thal, D.M. The impact of cryo-EM on determining allosteric modulator-bound structures of G protein-coupled receptors. *Curr Opin Struct Biol* **79**, 102560 (2023).
9. Stoddart, L.A., White, C.W., Nguyen, K., Hill, S.J. & Pfleger, K.D. Fluorescence- and bioluminescence-based approaches to study GPCR ligand binding. *Br J Pharmacol* **173**, 3028-3037 (2016).
10. Stoddart, L.A. et al. Application of BRET to monitor ligand binding to GPCRs. *Nat Methods* **12**, 661-663 (2015).
11. Milligan, G., Shimpukade, B., Ulven, T. & Hudson, B.D. Complex Pharmacology of Free Fatty Acid Receptors. *Chem Rev* **117**, 67-110 (2017).
12. Lin, D.C. et al. Identification and pharmacological characterization of multiple allosteric binding sites on the free fatty acid 1 receptor. *Mol Pharmacol* **82**, 843-859 (2012).
13. Srivastava, A. et al. High-resolution structure of the human GPR40 receptor bound to allosteric agonist TAK-875. *Nature* **513**, 124-127 (2014).
14. Kumari, P., Inoue, A., Chapman, K., Lian, P. & Rosenbaum, D.M. Molecular mechanism of fatty acid activation of FFAR1. *Proc Natl Acad Sci U S A* **120**, e2219569120 (2023).
15. Lu, J. et al. Structural basis for the cooperative allosteric activation of the free fatty acid receptor GPR40. *Nat Struct Mol Biol* **24**, 570-577 (2017).
16. Christiansen, E., Hudson, B.D., Hansen, A.H., Milligan, G. & Ulven, T. Development and Characterization of a Potent Free Fatty Acid Receptor 1 (FFA1) Fluorescent Tracer. *J Med Chem* (2016).
17. Branchini, B.R. et al. Sequential bioluminescence resonance energy transfer-fluorescence resonance energy transfer-based ratiometric protease assays with fusion proteins of firefly luciferase and red fluorescent protein. *Anal Biochem* **414**, 239-245 (2011).

18. Bertrand, R. et al. Synthesis and Characterization of a Promising Novel FFAR1/GPR40 Targeting Fluorescent Probe for beta-Cell Imaging. *ACS Chem Biol* (2016).
19. Ren, X.M. et al. Investigation of the Binding Interaction of Fatty Acids with Human G Protein-Coupled Receptor 40 Using a Site-Specific Fluorescence Probe by Flow Cytometry. *Biochemistry-Us* **55**, 1989-1996 (2016).
20. Ueno, H. et al. GPR40 full agonism exerts feeding suppression and weight loss through afferent vagal nerve. *PLoS One* **14**, e0222653 (2019).
21. Furukawa, H. et al. Design and Identification of a GPR40 Full Agonist (SCO-267) Possessing a 2-Carbamoylphenyl Piperidine Moiety. *J Med Chem* **63**, 10352-10379 (2020).
22. Christiansen, E. et al. Discovery of TUG-770: A Highly Potent Free Fatty Acid Receptor 1 (FFA1/GPR40) Agonist for Treatment of Type 2 Diabetes. *ACS Med Chem Lett* **4**, 441-445 (2013).
23. Ciba, M., Dibnah, B., Hudson, B.D. & Rexen Ulven, E. Development and Characterization of Potent Succinate Receptor Fluorescent Tracers. *J Med Chem* **66**, 8951-8974 (2023).
24. Ho, J.D. et al. Structural basis for GPR40 allosteric agonism and incretin stimulation. *Nat. Commun.* **9**, 1645 (2018).
25. Christiansen, E. et al. Free fatty acid receptor 1 (FFA1/GPR40) agonists: mesylpropoxy appendage lowers lipophilicity and improves ADME properties. *J Med Chem* **55**, 6624-6628 (2012).
26. Negoro, N. et al. Discovery of TAK-875: A Potent, Selective, and Orally Bioavailable GPR40 Agonist. *ACS Med Chem Lett* **1**, 290-294 (2010).
27. Tan, C.P. et al. Selective small-molecule agonists of G protein-coupled receptor 40 promote glucose-dependent insulin secretion and reduce blood glucose in mice. *Diabetes* **57**, 2211-2219 (2008).
28. Briscoe, C.P. et al. Pharmacological regulation of insulin secretion in MIN6 cells through the fatty acid receptor GPR40: identification of agonist and antagonist small molecules. *Br J Pharmacol* **148**, 619-628 (2006).
29. Hudson, B.D. Using Biosensors to Study Free Fatty Acid Receptor Pharmacology and Function. *Handb Exp Pharmacol* **236**, 79-100 (2017).
30. Johnstone, E.K.M. et al. Investigation of Receptor Heteromers Using NanoBRET Ligand Binding. *Int J Mol Sci* **22** (2021).
31. Toy, L., Huber, M.E., Schmidt, M.F., Weikert, D. & Schiedel, M. Fluorescent Ligands Targeting the Intracellular Allosteric Binding Site of the Chemokine Receptor CCR2. *ACS Chem Biol* **17**, 2142-2152 (2022).
32. Ruigrok, H.J. et al. Full-Spectral Multiplexing of Bioluminescence Resonance Energy Transfer in Three TRPV Channels. *Biophys J* **112**, 87-98 (2017).
33. Breton, B. et al. Multiplexing of multicolor bioluminescence resonance energy transfer. *Biophys J* **99**, 4037-4046 (2010).
34. Carriba, P. et al. Detection of heteromerization of more than two proteins by sequential BRET-FRET. *Nat Methods* **5**, 727-733 (2008).
35. Machleidt, T. et al. NanoBRET-A Novel BRET Platform for the Analysis of Protein-Protein Interactions. *Acs Chemical Biology* **10**, 1797-1804 (2015).
36. Kimura, I., Ichimura, A., Ohue-Kitano, R. & Igarashi, M. Free Fatty Acid Receptors in Health and Disease. *Physiol Rev* **100**, 171-210 (2020).

37. Hauge, M. et al. GPR40 (FFAR1) - Combined Gs and Gq signaling in vitro is associated with robust incretin secretagogue action ex vivo and in vivo. *Mol Metab* **4**, 3-14 (2015).
38. May, L.T., Leach, K., Sexton, P.M. & Christopoulos, A. Allosteric modulation of G protein-coupled receptors. *Annu Rev Pharmacol Toxicol* **47**, 1-51 (2007).

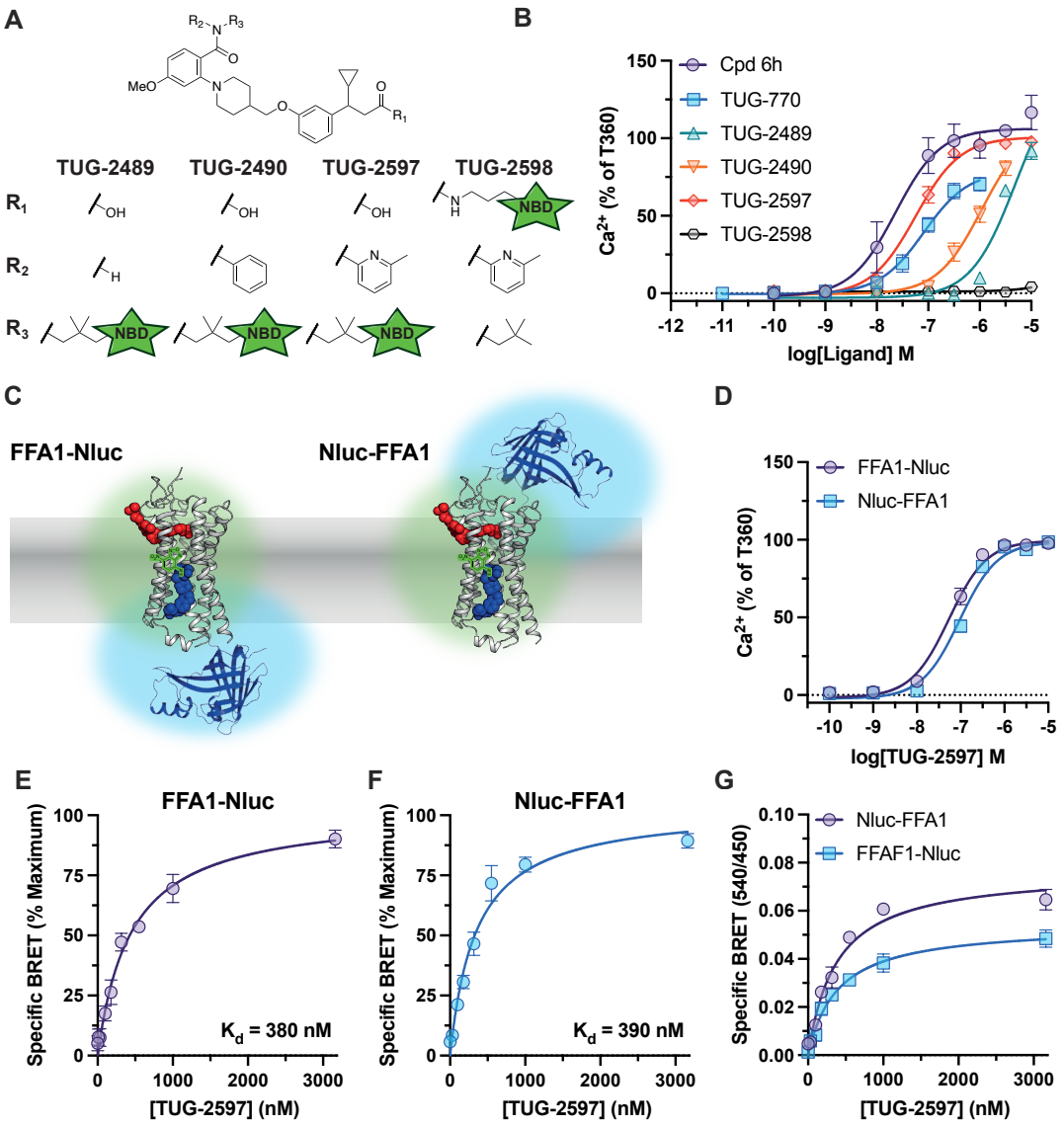

Figure 1. *Development of TUG-2597, a green fluorescent tracer binding to FFA1 site two.* **A**. Chemical structures of putative site two fluorescent tracers based on Cpd 6h. The linkers used and the position of an NBD green fluorophore are shown. **B**. The activity of putative fluorescent tracers at FFA1 were assessed in Ca^{2+} mobilisation assays and compared to FFA1 site two (Cpd 6h) and site one (TUG-770) reference ligands. Data are from N=3 independent experiments and normalized against the response to T360. **C**. The proximity between the NBD tag of TUG-2597 (blue spheres) and Nluc is predicted to be sufficient for BRET to occur both with the Nluc tagged either at the C (left) or N (right) terminal of FFA1, shown with overlapping green and blue spheres in the illustration. A site one ligand is shown with red spheres. **D**. Comparison of Ca^{2+} responses to TUG-2597 in cells expressing FFA1 tagged at its N or C terminal with Nluc. Data are from N=3 independent experiments and normalized against the response to T360. Specific BRET binding curve for TUG-2597 obtained in cells expressing an FFA1 construct tagged at its C (**E**) or N (**F**) terminal with Nluc are shown. Specific BRET was determined by subtracting non-specific BRET binding obtained in the presence of the competing ligand, T360 (10 µM). Data are expressed as a percentage of the maximal signal. **G**. Saturation BRET binding curves for TUG-2597 are compared between the C terminal and N terminal FFA1 constructs. Data are shown as the BRET ratio (540 nm / 450 nm emission). Saturation binding experiments (**E-G**) are from N=3 independent experiments.

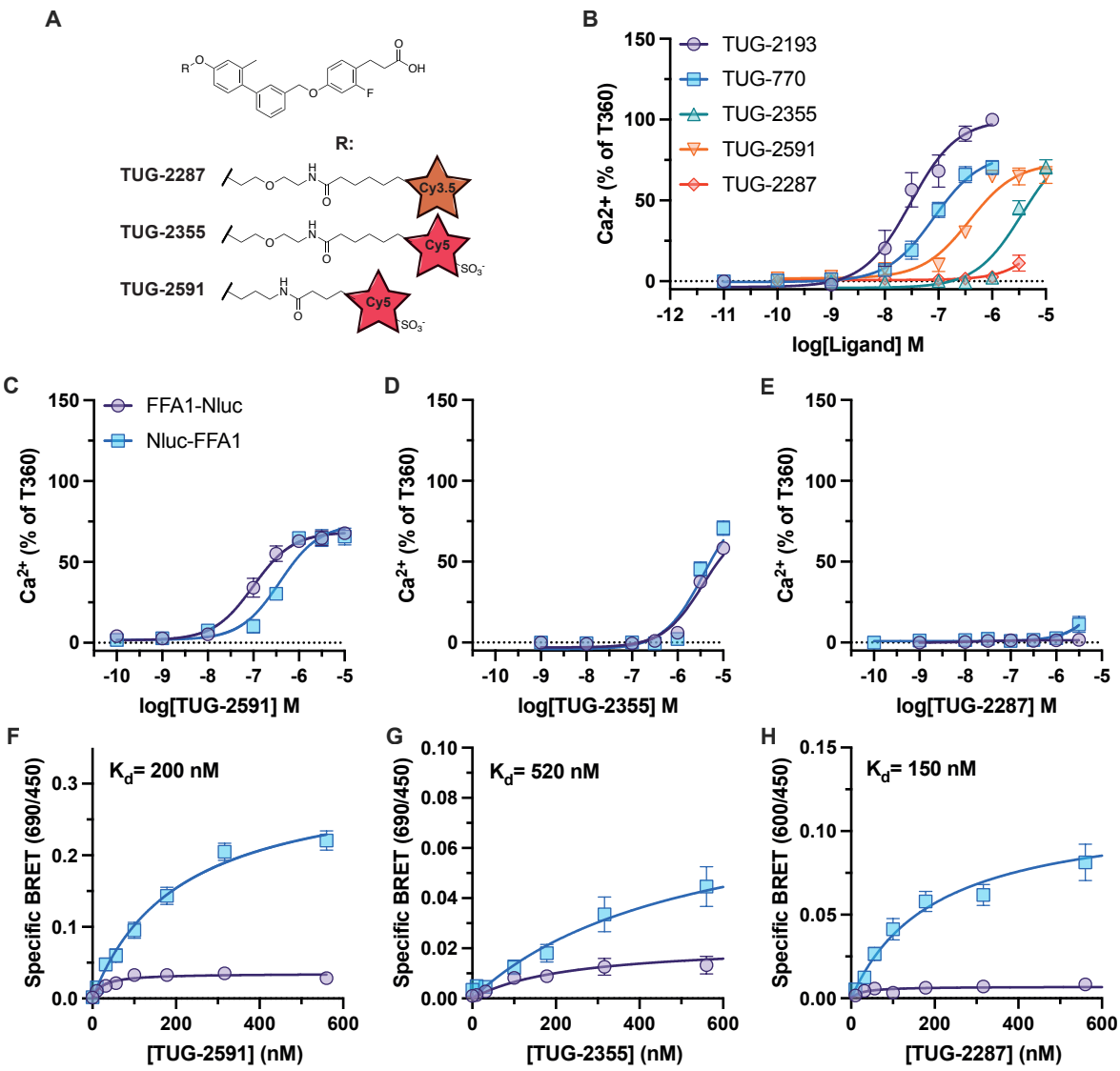

***Figure 2**. Identification of TUG-2591 as a red fluorescent tracer binding to FFA1 site one*. **A**. Chemical structures of putative red fluorescent tracers for site one of FFA1. Compounds are based on a previously described green tracer, TUG-1460, with the linkers used as well as the position and identity of the red fluorophore shown. **B**. The activity of putative fluorescent tracers at FFA1 were assessed in Ca^{2+} mobilisation assays and compared to Cpd 6h (site two) and TUG-770 (site one) reference ligands. Data are from N=3 independent experiments and normalized against the response to T360. The ability of the three putative red tracers, TUG-2591 (**C**), TUG-2355 (**D**), and TUG-2287 (**E**) to produce a Ca^{2+} mobilisation responses are shown comparing responses in cells expressing FFA1 tagged at its C (purple, circles) or N (blue, squares) terminal with Nluc. Data in **C-D** are from N=3 independent experiments and normalized against the response to T360. Saturation BRET binding experiments compare specific BRET obtained from the C (purple, circles) or N (blue, squares) terminal FFA1 Nluc constructs with TUG-2591 (**F**), TUG-2355 (**G**), and TUG-2287 (**H**). Specific BRET was calculated by subtracting non-specific BRET binding obtained in the presence of the competing ligand, TUG-770 (10 μM). Saturation binding experiments **(F-H)** are from N=3 independent experiments.

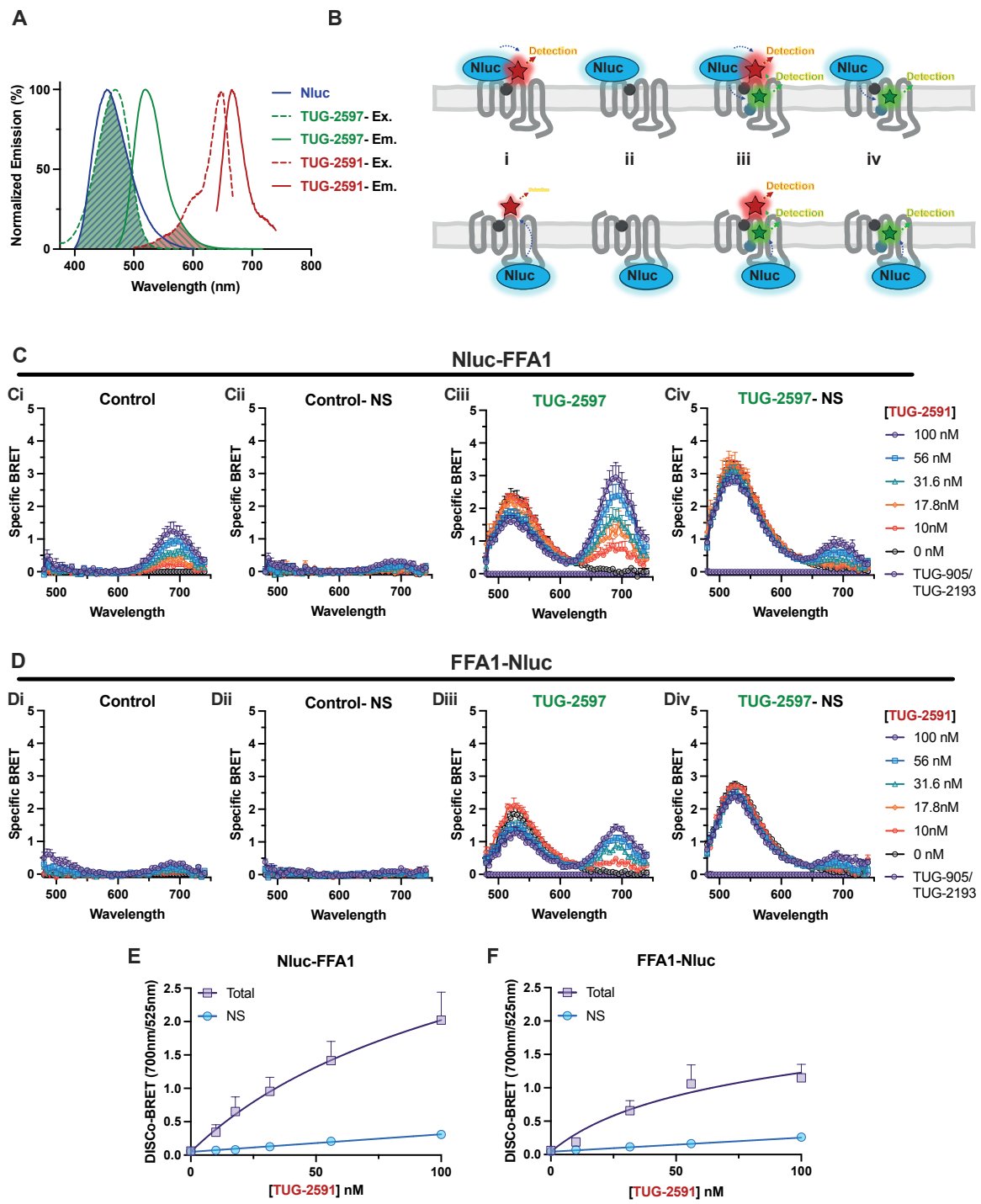

***Figure 3**. Dual Interaction Sequential Compound (DISCo)-BRET measures simultaneous binding of tracer ligands to two distinct FFA1 binding sites*. **A**. The spectral properties of Nluc, TUG-2591 and TUG-2597 are shown. Spectral overlap in Nluc emission with TUG-2597 excitation, as well as overlap in TUG-2597 emission with TUG-2591 excitation are highlighted. **B**. A cartoon diagram demonstrates predicted BRET energy transfer between Nluc, a red site one tracer and a green site two tracer. The cartoons depict the experimental conditions used incubating Nluc-FFA1 or FFA1-Nluc cells with: i) the red site one tracer alone; ii) the red site one tracer combined with a competing ligand; iii) the red site one tracer and the green site two tracer; and iv) the red site one tracer, the green site two tracer and a competing ligand for site one. **C**. Luminescent emission spectra were recorded from cells expressing an N terminally Nluc tagged FFA1 with

increasing concentrations of the red tracer TUG-2591. All spectra are shown as 'specific BRET' by subtracting the spectrum obtained in the presence competing ligands for both allosteric site one and two, TUG-905 (10 μM) and T360 (10 μM). Data are shown for the control condition (**Ci**); for the control non-specific (NS) condition, in the presence of TUG-770 to show non-specific TUG-2591 binding (**Cii**); in the presence of 316 nM of the green tracer TUG-2597 (**Ciii**); or non-specific binding in the presence of TUG-2597, with both 316 nM TUG-2597 and 10 μM TUG 905 (**Civ**). **D**. Comparable experiments to those presented in **C** were conducted using cells expressing an FFA1 construct with Nluc fused to the C terminal of the receptor. DISCo-BRET saturation binding curves showing total and non-specific (in the presence of 10 μM TUG-905) TUG-2591 binding in the presence of TUG-2597 at either N (**E**) or C (**F**) terminal Nluc tagged FFA1 constructs are shown. DISCo-BRET was calculated by taking the area under the SulfoCy5 peaks (660-730 nm) divided by the area under the NBD peaks (490-560 nm) from the specific BRET spectra shown in **C** and **D**. All DISCo-BRET data shown are from N=4 independent experiments.

Figure 4

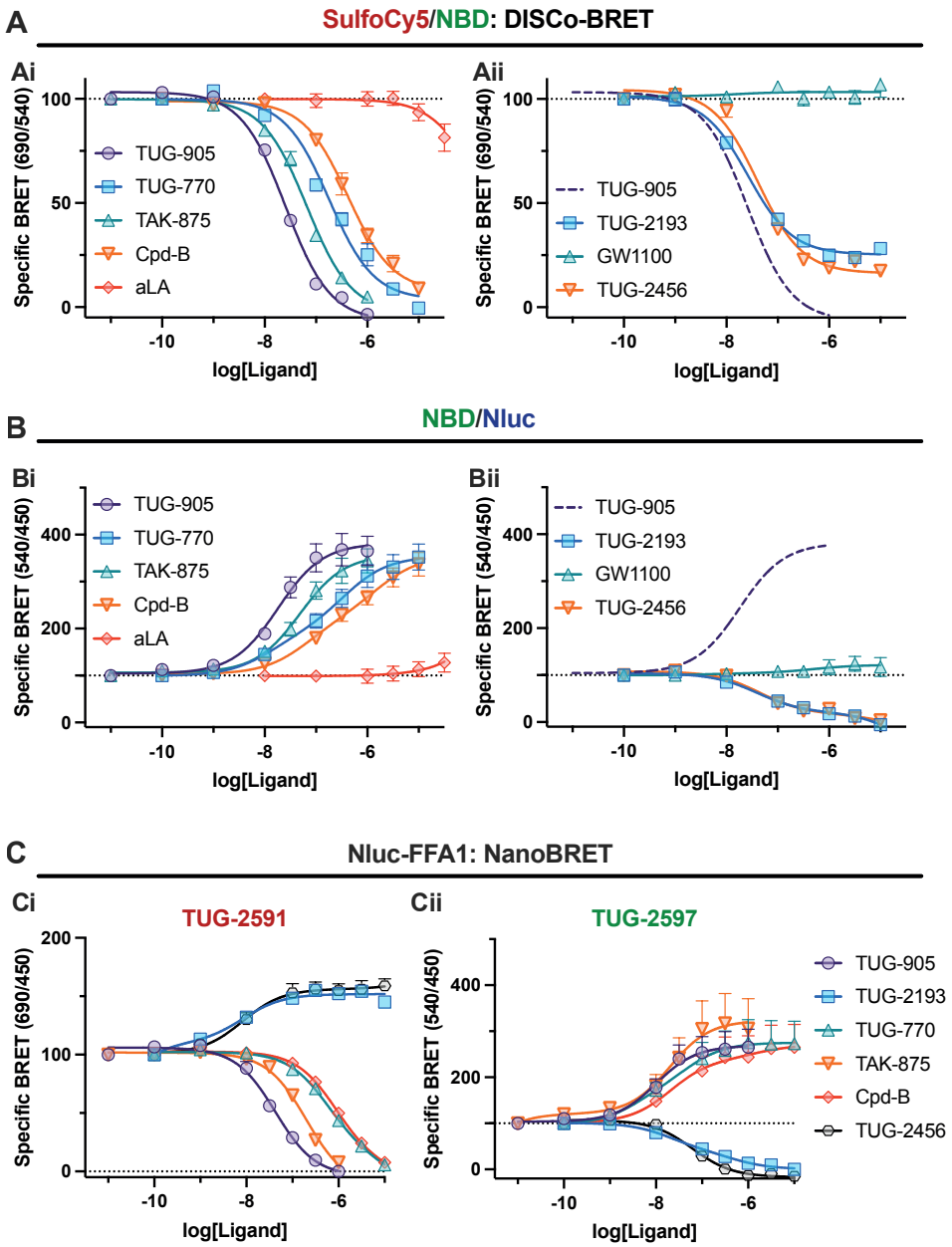

***Figure 4**. DISCo-BRET competition binding experiments identify ligands binding to the two distinct FFA1 allosteric binding sites*. Competition DISCo-BRET binding experiments were conducted in the presence of both the red tracer TUG-2591 (100 nM) and the green tracer TUG-2597 (316 nM). Data are shown as the ratio of 690 nm / 540 nm luminescent emission (**A**), or 540 nm / 450 nm luminescent emission (**B**) and expressed as specific BRET above that obtained in the presence of both competing ligands, TUG-905 (10 μM) and TUG 2193 (10 μM). Competition binding data with various compounds are split over two graphs (**i** and **ii**), with the curve for TUG-905 shown as a dashed line in **ii** for reference. DISCo-BRET competition experiments data are from N=4-7 experiments. NanoBRET competition binding experiments using the N terminal Nluc tagged FFA1 construct and either 100 nM TUG-2591 (**Ci**) or 316 nM TUG-2597 (**Cii**) are shown. Specific binding is shown after subtracting BRET obtained with 10 μM TUG-905 (**Ci**) or 10 μM T360 (**Cii**). NanoBRET data are from N= 3-4 independent experiments.

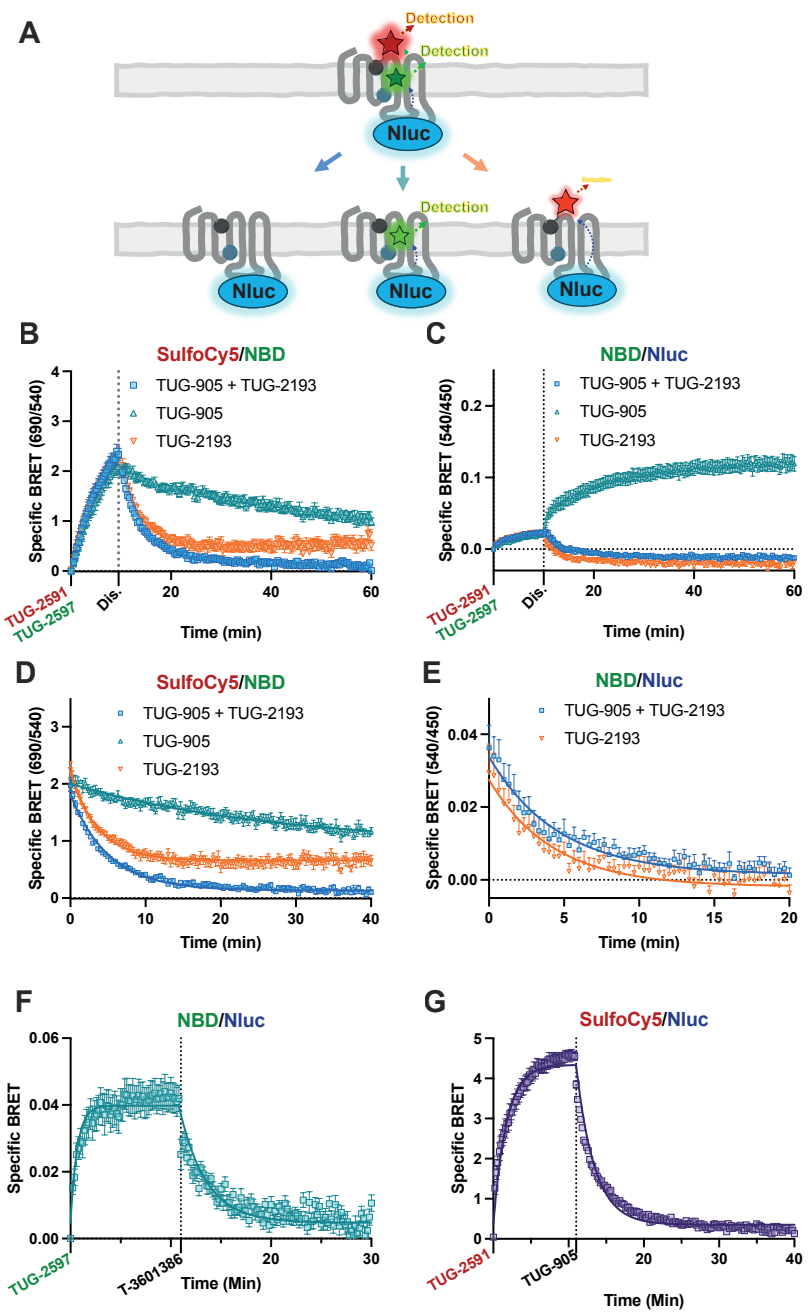

***Figure 5**. DISCo-BRET kinetics reveals slow off rate at allosteric site one when a compound is bound to allosteric site two*. **A.** A cartoon diagram depicting a DISCo-BRET dissociation-rate experiment. Receptor was pre bound to both the red and green tracers, followed by addition of a competing ligands for both site one and site two (left), site one alone (middle), or site two alone (right). Experiments were conducted where cells were first treated with TUG-2591 (100 nM) and TUG-2597 (316 nM) together, before the addition (marked as Dis.) of TUG-905 (10 μM), T360 (10 μM) or a combination of TUG-905 and T360 (10 μM each) to assess the dissociation of the FFA1/ TUG-2591/ TUG-2597 complex. Data from these experiments are shown as the 690 nm / 540 nm (**B**), or 540 nm / 450 nm (**C**) luminescent emission ratios. **D**. The dissociation portion of the curve from **B** is plotted and fit to a one site exponential decay model. **E**. The dissociation portion of the curve from **C** is plotted and fit to a one site exponential decay model. Dissociation NanoBRET experiments are shown for TUG-2591 (**F**) and TUG-2597 (**G**), following treatment with TUG-905 (10 μM) and T360 (10 μM) respectively. NanoBRET data (**F-G**) are from N=3 independent experiments.

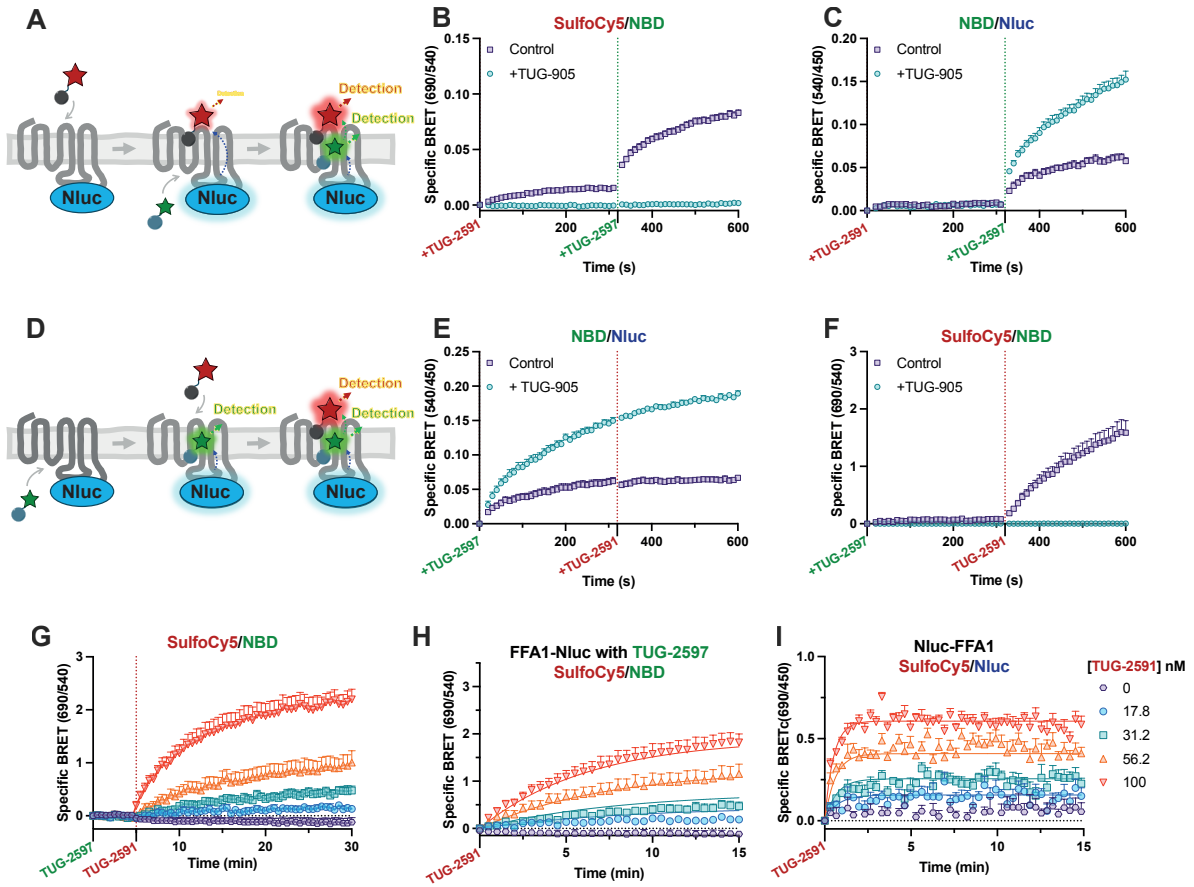

Figure 6. *DISCo-BRET demonstrates significantly slower on-rate kinetics at FFA1 site one when a compound is bound to site two.* Sequential bind experiments were conducted by treating first with red TUG-2591 (300 nM), then with green TUG-2597 (316 nM) (**A**), and data were plotted as either the 690 nm / 540 nm (**B**) or the 540 nm / 450 nm (**C**) luminescent emission ratios. Experiments were carried out either as control experiments or in the presence of TUG-905 (10 μM) to prevent binding of TUG-2591. Specific BRET was obtained by subtracting the non-specific BRET ratio obtained in cells that had been pre-treated with both TUG-905 (10 μM) and T360 (10 μM). Comparable sequential binding data are shown (**D-E**) when cells treated first with TUG-2597 (316 nM), then with TUG-2591 (100 nM). Data from sequential binding experiments are presented from N=3-5 independent experiments. **G**. Sequential binding experiments adding first TUG-2597 (316 nM) followed by increasing concentrations of TUG-2591. Data are from N=3 independent experiments. **H**. The TUG-2591 association portion of these experiments are isolated and fit to a multiple concentration of labelled ligand binding association model. **I**. Comparable NanoBRET association experiments using an N terminal Nluc tagged FFA1 construct and multiple concentrations of TUG-2591 are fit to a multiple concentration of labelled ligand binding association model. Data are from N=4 independent experiments.